NAVAL POSTGRADUATE SCHOOL
Monterey, California

THESIS

Target Identification Algorithm for the AN/AAS-44V Forward Looking Infrared (FLIR)

by

Jessica Herman

June 2000

Thesis Advisor: Neil C. Rowe
Second Reader: Wolfgang Baer

Approved for public release; distribution is unlimited

REPORT DOCUMENTATION PAGE		Form Approved OMB No. 0704-0188

Public reporting burden for this collection of information is estimated to average 1 hour per response, including the time for reviewing instruction, searching existing data sources, gathering and maintaining the data needed, and completing and reviewing the collection of information. Send comments regarding this burden estimate or any other aspect of this collection of information, including suggestions for reducing this burden, to Washington headquarters Services, Directorate for Information Operations and Reports, 1215 Jefferson Davis Highway, Suite 1204, Arlington, VA 22202-4302, and to the Office of Management and Budget, Paperwork Reduction Project (0704-0188) Washington DC 20503.

1. AGENCY USE ONLY *(Leave blank)*	2. REPORT DATE June 2000	3. REPORT TYPE AND DATES COVERED Master's Thesis
TITLE AND SUBTITLE : Target Identification Algorithm for the AN/AAS-44V Forward Looking Infrared (FLIR)		5. FUNDING NUMBERS
6. AUTHOR(S) Herman, Jessica L.		
7. PERFORMING ORGANIZATION NAME(S) AND ADDRESS(ES) Naval Postgraduate School Monterey, CA 93943-5000		8. PERFORMING ORGANIZATION REPORT NUMBER
9. SPONSORING / MONITORING AGENCY NAME(S) AND ADDRESS(ES) N/A		10. SPONSORING / MONITORING AGENCY REPORT NUMBER

11. SUPPLEMENTARY NOTES The views expressed in this thesis are those of the author and do not reflect the official policy or position of the Department of Defense or the U.S. Government.

12a. DISTRIBUTION / AVAILABILITY STATEMENT Approved for public release; distribution is unlimited.	12b. DISTRIBUTION CODE

ABSTRACT *(maximum 200 words)*

Accurate identification of unknown contacts is a crucial issue in military intelligence. In order for this task to be accomplished by human observers, each one must be specially trained and regularly re-qualify. Even with training, their decisions are subject to human error: bias, expectations, or even a lack of sleep may compromise their accuracy. If an automated system could quickly and accurately determine the identity of a contact, it would be a great benefit. This thesis explores some of the problems which must be addressed in producing such a system. We detail an approach to an algorithm which compares a picture of an unknown ship to an established database and determines its most likely classification. In particular, we use infrared images from FLIR video taken at sea, and obtain classification results for a small test set. We tested eighteen images with success rates varying between seventy-three and eighty-nine percent.

14. SUBJECT TERMS Image recognition, ship identification, Hough transform, edge detection			15. NUMBER OF PAGES 70
			16. PRICE CODE
17. SECURITY CLASSIFICATION OF REPORT Unclassified	18. SECURITY CLASSIFICATION OF THIS PAGE Unclassified	19. SECURITY CLASSIFICATION OF ABSTRACT Unclassified	20. LIMITATION OF ABSTRACT UL

NSN 7540-01-280-5500

Standard Form 298 (Rev. 2-89)
Prescribed by ANSI Std. 239-18

THIS PAGE INTENTIONALLY LEFT BLANK

Approved for public release; distribution is unlimited.

Target Identification Algorithm for the AN/AAS-44V Forward Looking Infrared (FLIR)

Jessica L. Herman
Ensign, United States Navy
B.S., Stanford University, 1999

Submitted in partial fulfillment of the
requirements for the degree of

MASTER OF SCIENCE IN COMPUTER SCIENCE

from the

NAVAL POSTGRADUATE SCHOOL
June 2000

Author: 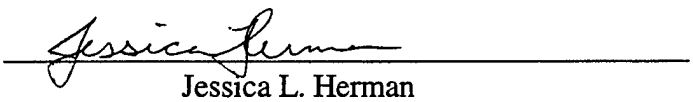
Jessica L. Herman

Approved by: 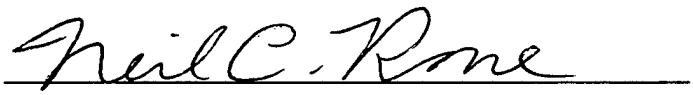
Neil Rowe, Thesis Advisor

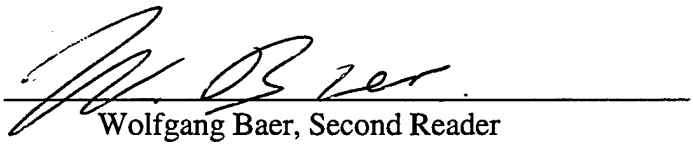
Wolfgang Baer, Second Reader


Daniel Boger, Chairman
Department of Computer Science

THIS PAGE INTENTIONALLY LEFT BLANK

ABSTRACT

Accurate identification of unknown contacts is a crucial issue in military intelligence. In order for this task to be accomplished by human observers, each one must be specially trained and regularly re-qualify. Even with training, their decisions are subject to human error: bias, expectations, or even a lack of sleep may compromise their accuracy. If an automated system could quickly and accurately determine the identity of a contact, it would be a great benefit. This thesis explores some of the problems which must be addressed in producing such a system. We detail an approach to an algorithm which compares a picture of an unknown ship to an established database and determines its most likely classification. In particular, we use infrared images from FLIR video taken at sea, and obtain classification results for a small test set. We tested eighteen images with success rates varying between seventy-three and eighty-nine percent.

THIS PAGE INTENTIONALLY LEFT BLANK

I. INTRODUCTION

Image recognition methods are applicable to a wide range of problems in both the military and civilian world. A number of techniques have been utilized in everything from robot assembly lines to identifying tanks in satellite pictures. Much of the research thus far, however, has been restricted to artificially designed problems in which the test images are carefully selected or constructed. In order to build a useful combat system, a method is required which is robust enough to be used on real images.

The task of identifying unknown contacts at sea (ships sighted) is currently delegated to trained human observers. Personnel must undergo extensive training in order to meet the Navy's need for accurate identification. They must be regularly retrained as these skills deteriorate quickly. In addition, human judgment can be biased by any number of factors. If a computer system could be designed to reliably and accurately perform this function, these problems could be significantly reduced, leading to better and more efficient performance.

This thesis is the first step in developing an image analysis module for the Maritime Analysis Recognition Knowledge System (MARKS) proposed by Lt. Matthew Lisowski, USN. MARKS is a design for a platform-independent ship-identification system which will integrate regional data, emitter analysis, and image analysis to provide fast, accurate classification of unknown contacts. Each module will provide confidence ratings for the most likely candidates, which will be combined by the system to determine the identity of the contact. The image analysis module will operate on a database which is pruned by regional information to contain only nearby ships. It will then further narrow

the choices by comparing an image of the unknown ship to those in the database, and will return the most probable identification and a measure its similarity.

Our image analysis module operates on a screen capture from infrared (specifically, Forward-Looking Infrared, FLIR) video. We require the shots to be close to broadside, and the entire ship must be within the image boundary. Otherwise, we attempt to accommodate as much of the normal appearance of the FLIR images as possible. System information projected onto the image (such as crosshairs and range information) is eliminated by the program's pre-processing phase, and small variations in location and orientation of the ship are recognized. We then construct a feature vector which efficiently represents the important characteristics of the ship. This representation is compared to the feature representations of all the ships in the database using a standard distance calculation. The distances between the ship to be identified and those in the database become the confidence ratings by which the classification can be done.

In this thesis, we examine the problems of implementing an algorithm for identifying ships from FLIR video. We first review the literature pertaining to our topic, then describe the program we designed as a possible approach to this problem and its performance. Finally, we discuss the implications of our work and the continuing research it suggests.

II. BACKGROUND

A. OVERVIEW

The task of image recognition, whether by computer or by human being, can be broken into three distinct phases. First, the observer extracts relevant data out of the scene. This may include separating foreground from background, registering color and texture, or locating edges. Next, semantic information is imposed on the raw data. Areas are numbered, angles are measured, features are labeled, and so on. By imposing structure, the image is transformed into a set of facts for use in a third stage of classification. In this step, the accumulated knowledge is used to determine the identity or properties of the target object.

Our focus in this thesis is on the first part of the recognition process. We use a simple similarity metric to classify images. In chapter 6, we give some suggestions on how our accuracy might be improved by using more advanced techniques in the analysis and classification stages.

B. IMAGE RECOGNITION

Prior studies on image recognition have employed a wide range of disparate techniques. No one method emerges from this field as generally superior for all problems. The most commonly applied approaches, however, fall into three broad categories. Pattern-matching systems search for particular patterns such as shapes or angles in an image, and use these as a basis for comparison. A number of different mathematical transformations can be applied to images, edge images, or silhouettes to

generate a new image in transform space which is easier to analyze. The final set of methods includes those which extract information from properties of the whole input image, such as moment analysis and some uses of artificial neural networks.

1. Pattern Matching: Bump-finding

Searching for particular shapes can be very effective when the image domain is well-defined. [Ref. 1] presents a method for identifying ships based on the decomposition of "bumps" on their decks. The theory is based on the common rule-based training students are given when learning to differentiate ship classes. Each class is defined by the structures it contains and their arrangement on the deck. This forms a rule: A given pattern of structures implies that a ship is of a particular type. Students then memorize all types of structures, and apply the rules to determine ship types.

The goals of this study were to isolate bumps on a ship's deck and to accurately determine their identities. Silhouettes obtained from [Ref. 2] were searched for locations where the outline made an upward turn. Each of the areas defined by such turns was further analyzed in the same way in order to develop a model of the whole bump. Finally, the model was identified using a rule-based system. The program found and classified the protrusions with an average accuracy of 78%.

This work could be easily extended to identify ships from the pattern of bumps. Another set of rules could be constructed to determine what class of ship most closely matched the current configuration of features. The usefulness of this method is restricted, however, by its dependence on detailed, clear silhouettes. A noisy image, or one in which the edge of the ship was not continuous, could not be successfully processed. The time

and space required to identify even these few features also limits the scalability of the technique.

2. Transforms: Hough Transform

The Hough transform was developed to detect straight lines in images. Its popularity is largely due to its ability to operate on noisy or incomplete images, which makes it well suited to our problem. While we use the transform as an aid in finding straight lines, it is possible to make direct comparisons in transform space, as shown in [Ref. 3].

This study proposed a method for locating and recognizing arbitrary two-dimensional shapes. First, the features of the shape to be identified are extracted from a training image. The shape is placed at a reference position and orientation, and then the Hough transform is applied. Peaks in parameter space are identified, and their pattern is stored.

To locate the training shape in a test image, the pattern of peaks in parameter space is computed as above. The one-dimensional convolution of angle histograms for the training and test peak patterns is calculated. This function's highest peak gives the orientation of the shape in the test image. Once the angle of rotation is determined, the patterns can be searched for corresponding peaks. The translational displacement can also be found by a three-point comparison of significant peaks.

The proposed method was able to successfully locate and confirm shapes made up of straight lines, independent of rotation and translation. A scale-invariant extension was also suggested. A number of other studies have also designed extensions for the Hough

transform [Refs. 4, 5] or methods involving other transforms [Ref. 6] for various recognition tasks.

We attempted to use a similar technique on our FLIR images, but without success. Calculations on the raw Hough transform are difficult and computationally expensive to extend to complex shapes, especially in noisy images with varying scale, translation and rotation. Additionally, since we are trying to classify a ship rather than to find a known shape, the costly matching process would have to be done for each possible ship type.

3. Entire-image Operations: Moments

In [Ref. 7], an experimental system for recognizing aircraft from optical images is described. The aim of this research was to classify images of military aircraft by use of rotation-, translation- and scale-invariant functions. One type of function which meets these criteria is a moment-invariant. The authors defined a set of moment-invariant functions based on the second- and third-order moments of the image silhouette, and used them for classification.

Images for this study were obtained by photographing white model airplanes against a black background, then applying a thresholding operation to produce a binary image. Six types of aircraft were compared using two separate classification methods, one based on a nearest-neighbor calculation, and the other on probability estimation using Bayes' Rule.

This system produced highly accurate results: fewer than 10 of 132 test images were incorrectly matched. It also ran quickly in classification mode. It is much more difficult, however, to handle more than six classes and it is questionable whether the method can be extended to use images of objects in natural contexts. Current research at the Naval Postgraduate School is applying moment-invariants to FLIR image identification. Other work has illustrated the merits of different entire-image techniques, such as dominant point detection [Ref. 8] and improved edge-detection [Ref. 9].

C. AERIAL PHOTOGRAPHY

Many object recognition techniques are also applied in other areas of image processing. The code we used to find line segments in our images is a modified form of a function from [Ref. 10]. Although our purpose was very different from that study, we shared low-level processing issues.

The proposed system compares grayscale aerial photographs to views generated from an existing database. Images are searched for landmarks, which are used to find a transformation to map one image onto the other. Once the images have been aligned, a differencing technique is used to find regions that have changed significantly since the database was last updated.

The segment finding procedure that we use is part of the differencing function. Straight lines are identified and grouped by the objects they represent. Lines in the new image that do not correspond to anything in the terrain database provide evidence for a new structure or road; lines from the database which do not appear in the new image indicate that some object has been removed.

THIS PAGE INTENTIONALLY LEFT BLANK

III. APPLICATION

A. PROJECT GOALS

In trying to design an algorithm with the potential for use in a combat system, we had to formulate requirements additional to those of most current recognition systems. We wanted our program to run efficiently in the classification phase so that as we increased the size of the database, identification could still be done in real time. The segmentation portion of the program also needed to run quickly. Clearly, we could not use artificially generated images since we were trying to identify ships from real FLIR video.

Our approach was also unusual in that we combined some of the standard techniques for recognition in new ways. To locate the ship in the image, we used edge detection, thresholding, and our prior knowledge of the domain. We extracted line segments by applying knowledge of Hough transform space features to our edge image. In the classification stage, we calculated moments and other statistical features both on line segments and directly on image pixels. By employing different methods on different tasks, we hoped to come up with a better solution than any individual process could provide.

B. DOMAIN ISSUES

We used a video capture card to obtain frames from footage taken by the crew of a SH-60B Rapid Deployment Kit equipped helicopter. The AN/AAS-44V FLIR is mounted on a springboard at the nose of the aircraft.

Because we used real FLIR images as our data, we dealt with a number of challenges in the pre-processing phase. We limited our samples to pictures in which the entire ship was visible and centered, and only used near-broadside views. Even with these requirements, the scale, position, and orientation of the ship varied significantly between images. The quality of the images was not ideal; we employed techniques to eliminate as much noise and background information from our samples as possible. To be cost-effective, an automated identification system needs to be able to operate on noisy data.

In addition to the problems that always arise when using real data, our images contained artifacts of the FLIR system from which they were obtained. The system projects video information and targeting aids onto the screen, as shown in Figure 1. These may partially obscure the image and interfere with the identification process. We tested the efficacy of a number of methods in removing these factors.

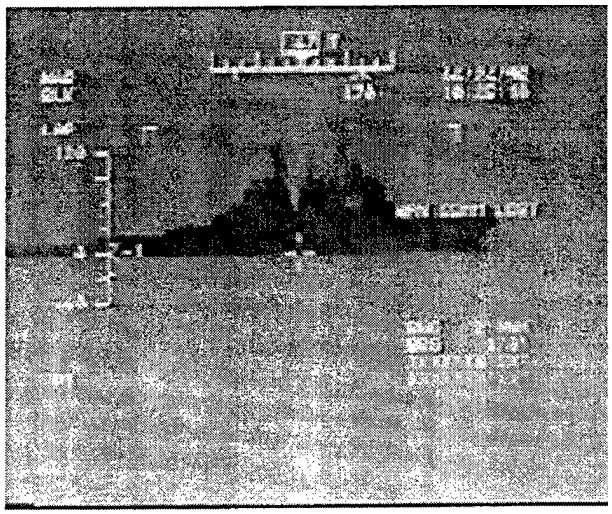

Figure 1.

The FLIR camera can be operated in a number of modes. It can display either black-hot (higher energy areas are black) or white-hot images, and provides both digital and optical zoom capabilities. We chose to use only black-hot images because we can more effectively remove system artifacts from them than from white-hot images. We also decided not to allow images produced with the digital zoom option, as it amplifies background noise significantly.

C. PROGRAM INPUT/ OUTPUT

Our program operates on images captured from FLIR video using a Studio PCTV. This system returns a 320 x 240 pixel TIFF format color image. The program's second input argument is a database which contains the comparison information for each possible ship class.

The program returns an ordered list of the ships in the database that are closest to the unknown ship. Each potential classification has a confidence rating which represents how similar the test image is to that class. We list multiple possibilities because if the

test image is very close to more than one database class, we want the system user to be aware of all strong possibilities. In the MARKS system, comparing our results with the results from the emitter and ship positioning systems will further narrow the database of candidate classes.

D. DESIGN DECISIONS

We chose to represent image data as a set of numerical features for three main reasons. First, we needed to reduce the amount of data in our comparisons between images if we wanted to produce an efficient, scalable system. We also wanted to make our program robust enough to operate on real pictures, so we had to find a way to avoid relying on exact data and to represent general properties of our images. Finally, making comparisons based on numbers is much easier than any other method. Using numerical features greatly simplified our classification step. By extracting important features from the images, we were able to make progress towards all of these goals.

Using straight line segments as our basic features fit well with our design objectives. Ship images consist mainly of straight lines, so most of the important information in our images is preserved. A line segment can also be represented succinctly by a few numbers: The coordinates of the center, the orientation, and the length fully describe it. This choice even helped us to reduce the noise in the images, as natural noise rarely produces straight lines as long and strong as those found in man-made objects.

IV. IMPLEMENTATION

A. PROGRAMMING ENVIRONMENT

We implemented our program in MATLAB (version 5.3.1.29215a) using the MATLAB Image Processing Toolbox. Because of its extensive image processing toolbox, MATLAB allowed us to concentrate on the high-level design aspects of the algorithm. If our algorithm were used in a real system, it could easily be translated into a more commonly used language such as C or Ada.

All of our research and testing were done on a Micron Millennia computer running Windows NT 4.0, so our run times are all for that platform.

B. APPROACH TO DOMAIN PROBLEMS

In order to reduce the impact of noise on our algorithm's performance, we combined multiple processing steps. During the pre-processing stage, we smoothed the images using standard median filtering on 3-by-3 pixel neighborhoods. Filtering reduced the graininess of the images so that fewer false edges were detected in the next step of segmentation, in which we located straight line segments in the edge image. The segmentation process itself eliminated many small regions of the image that resulted from noise, as we only dealt with line segments of significant length.

We applied the rest of our methods after segmentation. Our limitation to only black-hot images allowed us to remove all lines from the segmented images which mapped to light areas in the original images. Since the heat generated in the engines ensured that the ship would always be hot relative to the surrounding water, anything

'cold' (light in color) must be noise. We automatically generated a mask for each image to represent those pixels with light values, and removed those segments whose centers were within the mask from the edge image. This step also removed some of the processing artifacts, which were generally light. To deal with any that remained, we created another binary image that marked all of the areas where we knew such artifacts would be located. Then, as above, we disregarded all line segments that fell within those regions. Figures 2 and 3 show a segmented edge image (AB 1) before and after these processing steps.

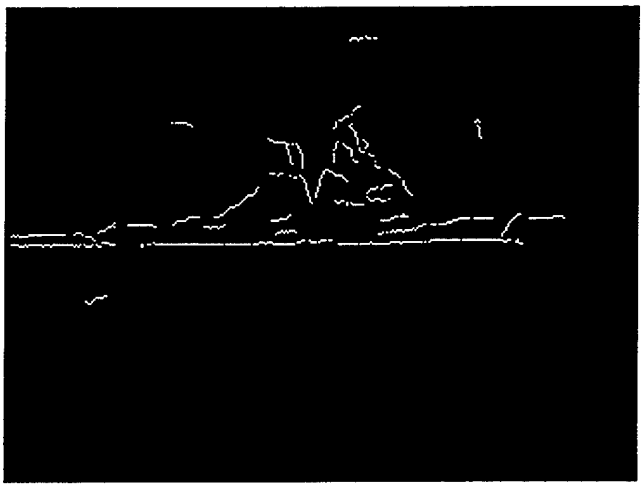

Figure 2.

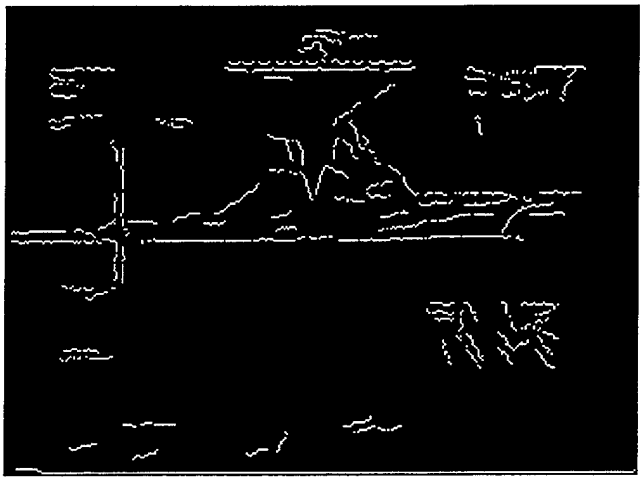

Figure 3.

We tested and discarded a few other techniques for the removal of spurious edges. Neighborhood averaging of light-colored pixels in the original intensity image, which we hoped would eliminate many spurious edges, did not accomplish anything useful. We tried smoothing areas that were part of a similar mask to the one discussed above, also without success. Finally, we tried to subtract the mask from the edge image before the segmentation step, with the result that we were unable to detect many key segments. Since none of our attempts to clean up the images before segmentation were successful, we were forced to apply the post-processing techniques discussed above. These required additional processing of the segment list as well as of the resulting image; fortunately, the impact on program efficiency was minimal.

C. FEATURE EXTRACTION

After converting an image to grayscale and smoothing it, we searched for strong candidate line segments to use in classification. First, we ran the image through an edge detector. This process determines which pixels in a grayscale image are on the boundary between two significantly different shaded regions. It returns a binary image the same size as the original image showing the locations of all edge pixels. We chose to use the Canny method for edge detection because it successfully found all of the important features in our images. We allowed MATLAB to automatically select the threshold for deciding whether or not a value change was significant.

Once all the edge pixels were located, we began the task of finding connected lines in the binary images. For this step, we used a modified version of the segment finding code from [Ref. 10]. This technique used the radon transform, which is the same

as the Hough transform in two dimensions, to detect straight lines. A peak in transform space maps to a line or lines in image space. See Appendix B for an explanation of the mathematics behind this technique. We found the peaks in the transform, which gave us the orientation of the strongest lines and their perpendicular distances from the center of the image.

When we had this information, we could find pixels on the lines corresponding to each peak, and connect pixels using the angle defined by the transform results. For each peak, we collected all of the pixels that we reached by simply looking for the next one nearby and at the correct angle. Each of these sets approximated a line segment. We ran this process twice, first with a higher threshold to extract major lines, and then again with a lower threshold to find smaller segments from the pixels which were not matched in the first pass. After this step, we had an image made up of numbered straight-line segments and a list of the endpoints, orientations, and lengths of each segment.

When all of the segments had been located, we applied the delayed pre-processing methods described in Section B to eliminate spurious edges caused by noise or FLIR projection information. This cleaned up both the image and the segment list. As part of this phase, we also determined the center coordinates of each segment, which we used later for statistical calculations. Next, we checked the orientation of the ship in the image to see if we ought to realign it. We used the radon transform for this step as well. Since the highest peak in transform space usually is the bottom of the ship because the waterline creates a strong straight edge, we looked at the orientation of that line and rotated the image to make it horizontal.

Finally, we removed any line segments that were on the edges of the image, as they are unlikely to be part of the ship and would interfere with our statistics. We found the y-axis standard deviation of edge pixels, and simply removed any line segments that fell more than two and a half standard deviations from the image's y-axis mean. The resulting binary image showed the important features of the ship with very few confounding factors.

D. FEATURE ANALYSIS

We calculated some simple statistics on the processed images to help us extract important features. To account for scale and translation between images, we first found the median and standard deviation of pixel locations for both x- and y-axes. Using this, twenty-five rectangular areas in the image were defined. The width of each area was one standard deviation as calculated along the x-axis, and the height was one standard deviation along the y-axis. We centered the first rectangle on the median image pixel, then added two more rows and columns in every direction, as shown in Figure 4.

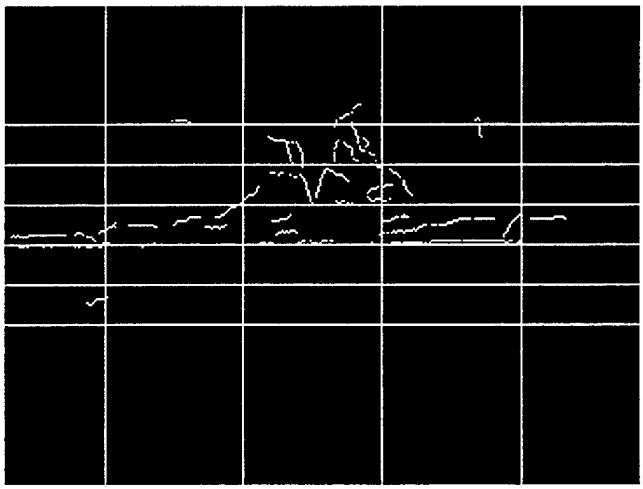

Figure 4.

For each of these ranges, we counted the number of pixels and then divided by the total number of edge pixels in the image. These measures gave a five-by-five array of fractions and showed how the pixels were distributed and thus gave the approximate shape of the ship. Next, we totaled the pixels in each box based on orientation. We defined four angle ranges, and for each area, counted the number of pixels which belonged to line segments in each angle range. Again, we divided the results by the total number of image edge pixels. This step resulted in a five-by-five-by-four array. We also calculated the third moment of the image pixel locations about the mean in the x and y directions (see Appendix B.) This feature measures skew or asymmetry, so it was helpful in distinguishing ship classes such as tankers and destroyers. The final form of our feature vector consisted of the two distribution arrays and the moment value, and contained a total of 126 elements.

E. ALGORITHM FOR CLASSIFICATION

To compare two segmented images, we first calculated the features described above. Next, we summed the absolute values of the differences between corresponding features of the two images. We used feature weights of 1, 10 and 5 for the pixel distribution, pixel orientation, and moment differences. These weights were chosen subjectively. The smaller the weighted sum of the absolute differences, the more alike the two images were judged.

V. RESULTS

A. IMAGES

We had a limited set of FLIR images for use in our tests. Consequently, we were not able to experiment with many different ship classes. Some of the images we did receive were too poor in quality to give good results. Our better images were of Arleigh Burke class destroyers and aircraft carriers. We had nine images of Arleigh Burkes and six images of carriers. Within those sets, the images varied enough to make identification difficult. In order to have more variety in our comparisons, we included two pictures of Spruance class destroyers in which the ships were small, as well as one very noisy picture of an Iranian PTG patrol craft.

B. ACCURACY

In our first trial, we computed the difference between each of our images separately. For each image, we found the feature difference from each other image. The results from this test are shown in Table 1. Since the difference function is commutative the table is symmetric about the diagonal. The difference between an image and itself is always zero, so those entries are left blank. Smaller differences indicate images which are more alike.

Table 2 summarizes the information in Table 1. For each image, we give the average difference between that image and the Arleigh Burke images, the carrier images, the Spruance images, and the patrol craft image. We also list the minimum image

	AB1	AB2	AB3	AB4	AB5	AB6	AB7	AB8	AB9	C0
AB1										
AB2	35.80									
AB3	58.74	48.17								
AB4	46.72	61.25	85.45							
AB5	46.53	40.78	34.43	69.01						
AB6	39.05	34.45	40.47	64.24	26.28					
AB7	20.84	34.23	57.41	41.60	42.29	34.98				
AB8	26.04	34.84	58.32	51.72	44.81	39.68	24.91			
AB9	39.38	36.55	41.07	64.85	26.14	19.50	37.29	43.23		
C0	67.83	63.84	31.70	93.35	39.85	47.09	65.33	62.46	47.94	
C1	34.54	31.69	55.88	62.04	45.30	36.15	34.96	30.61	39.83	57.88
C2	51.58	46.45	39.24	76.79	26.54	32.31	49.68	46.85	33.16	34.67
C3	66.99	61.67	31.12	91.95	41.40	48.01	64.93	60.43	49.22	21.73
C9	55.85	48.30	39.97	81.18	30.39	38.41	55.85	51.82	40.61	42.55
C10	90.07	80.77	54.11	115.40	64.49	72.55	90.81	86.53	73.00	50.00
DD1	75.51	85.04	111.77	43.57	98.62	91.50	71.72	77.66	94.54	117.66
DD2	32.51	42.48	68.95	57.52	55.99	49.19	32.51	30.59	52.85	70.37
PTG2	92.10	105.09	129.51	63.69	118.03	110.36	92.27	93.55	113.25	129.78

Table 1.

	C1	C2	C3	C9	C10	DD1	DD2
AB1							
AB2							
AB3							
AB4							
AB5							
AB6							
AB7							
AB8							
AB9							
C0							
C1							
C2	42.02						
C3	55.89	34.20					
C9	44.28	26.91	39.91				
C10	79.43	62.98	48.61	61.50			
DD1	84.36	99.36	114.00	96.24	135.02		
DD2	36.92	54.47	66.63	46.39	91.80	68.44	
PTG2	100.12	112.81	127.28	116.65	151.81	44.52	91.57

Table 1. (cont.)

difference and the image that produced it. The averages are taken over all images except the image to which they are being compared.

	AB avg	C Avg	DD Avg	PTG	Min	Min Ship
AB1	39.14	61.14	54.01	92.10	20.84	AB7
AB2	40.76	55.45	63.76	105.09	31.69	C1
AB3	53.01	42.00	90.36	129.51	31.12	C3
AB4	60.61	86.79	50.54	63.69	41.60	AB7
AB5	41.29	41.33	77.30	118.03	26.14	AB9
AB6	37.33	45.75	70.34	110.36	19.50	AB9
AB7	36.69	60.26	52.12	92.27	20.84	AB1
AB8	40.45	56.45	54.13	93.55	24.91	AB7
AB9	38.50	47.29	73.69	113.25	19.50	AB6
C0	57.71	41.37	94.01	129.78	21.73	C3
C1	41.22	55.90	60.64	100.12	30.61	AB8
C2	44.73	40.15	76.92	112.81	26.54	AB5
C3	57.30	40.07	90.32	127.28	21.73	C0
C9	49.15	43.03	71.31	116.65	26.91	C2
C10	80.86	60.50	113.41	151.81	48.61	C3
DD1	83.33	107.77	68.44	44.52	43.57	AB4
DD2	46.95	61.10	68.44	91.57	30.59	AB8
PTG2	101.98	123.07	68.04	---	44.52	D2

Table 2.

Out of the fifteen images that were of reasonably good quality (the Arleigh Burkes and the carriers), eleven (73%) were most similar to another ship in their class. When the class differences were averaged, however, thirteen of the fifteen (87%) were on average more similar to ships in the class to which they belonged. This result suggested that when we constructed a database to store data for multiple ship classes, we should average similarities over many views of the same ship class to classify a ship.

For another test, we selected one image from each ship class to put in the database. We chose the images that minimized the average difference to the rest of the

ships in their class, using the calculations in Table 2. All of the remaining images were then compared to these exemplars. The difference results are shown in Table 3.

	AB7	C3	DD1	PTG2
AB1	20.84	66.99	75.51	92.10
AB2	34.23	61.67	85.04	105.09
AB3	57.41	31.12	111.77	129.51
AB4	41.60	91.95	43.57	63.69
AB5	42.29	41.40	98.62	118.03
AB6	34.98	48.01	91.50	110.36
AB8	24.91	60.43	77.66	93.55
AB9	37.29	49.22	94.54	113.25
C0	65.33	21.73	117.66	129.78
C1	34.96	55.89	84.36	100.12
C2	49.68	34.20	99.36	112.81
C9	55.85	39.91	96.24	116.65
C10	90.81	48.61	135.02	151.81
DD2	32.51	66.63	68.44	91.57

Table 3.

Of the thirteen remaining good images (not counting the Spruance), two Arleigh Burkes and one carrier were incorrectly identified in this test, for a success rate of 77%. Since this was lower than the success rate when we averaged the class values in Table 2, we tried a new strategy.

We constructed feature vectors that were the average of the features over all images in each class with the exception of two test images, AB9 and C10. We then tested these two images against the vector averages. Our results are given in Table 4.

	AB avg	C avg	DD avg	PTG avg
AB9	37.15	39.25	76.24	113.25
C10	85.38	62.30	115.74	151.81

Table 4.

We repeated this process for eight other pairs of images (AB8/C9, AB7/C3, AB6/C2, AB5/C1, AB4/C0, AB3/C10, AB2/C9, and AB1/C3), building new feature vectors for each test which were averaged over the images not in the test set. Table 5 gives these results.

	AB avg	C avg	DD avg	PTG avg
AB8	35.85	60.87	55.59	93.55
C9	50.52	39.38	73.54	116.65
AB7	36.42	64.26	53.38	92.27
C3	59.90	33.33	92.39	127.28
AB6	37.38	48.88	73.08	110.36
C2	46.14	34.78	78.08	112.81
AB5	43.95	44.61	80.09	118.03
C1	30.41	57.72	61.75	100.12
AB4	66.90	89.70	35.50	63.69
C0	55.83	34.86	95.40	129.78
AB3	57.54	39.70	91.91	129.51
C10	88.65	62.30	115.74	151.81
AB2	29.35	58.51	64.91	105.09
C9	50.21	39.38	73.54	116.65
AB1	36.98	62.62	55.52	92.10
C3	60.20	33.33	92.39	127.28

Table 5.

Of our fifteen test images (we only counted each carrier image once even though we compared some of them twice), twelve (80%) were correctly identified. One of the mismatches, however, was with the Spruance class; since there were only two images in that group and neither was very good, that test was somewhat unfair. Ignoring it, the

percentage of accurate classifications between Arleigh Burkes and aircraft carriers was twelve of fourteen, or 89%.

C. SPEED AND EFFICIENCY

The most time-consuming portion of our program by far was the extraction of features from the original images. Each image required approximately 55 seconds for this step. Table 6 gives some example times in minutes and seconds for feature extraction.

AB1	0:55
AB2	0:40
AB3	1:00
C1	0:50
C2	1:00
C3	0:50

Table 6.

Constructing a big image-feature database will therefore be a lengthy process. Since the database can be put together offline, this is not a major concern; what matters more is the program's speed in recognition mode. When making 50 image-pair comparisons, the total time was less than one second, and for 100 comparisons, the time was still under three seconds. Thus a single comparison takes around three hundredths of a second.

Execution time could be reduced significantly by running our code on a faster computer. Translating our MATLAB code into a more efficient language would also give us a speed advantage.

THIS PAGE INTENTIONALLY LEFT BLANK

VI. CONCLUSIONS

A. SUCCESS OF PROJECT

This project achieved our major goals: Our segmentation step produces good results for most of our test images, and the recognition stage runs quickly and efficiently. We have certainly created a foundation on which further work can be built.

Our problems in finding FLIR images to work with limited our ability to fully test the system. We only had four types of ships, and in two of those classes the images were unusable due to noise and scale. The results from these trials are less meaningful than they would be if we had more variation in our data set.

The classification results were acceptable, but not perfect. This is to be expected, as we did not intend to focus on the classification stage. We designed a very simple feature space and difference measure to get some idea of whether our segmented images contained the relevant information to distinguish between ship classes. The features were really an approximation of the ships, rather than an accurate representation. With so few features, random statistical similarities between individual images sometimes outweighed general class similarities. That is largely why we had so many incorrect identifications in trials where individual ships were compared. Averaging features over classes ameliorated this problem somewhat, but only increasing the number of features can really solve it.

B. SUGGESTIONS FOR FUTURE RESEARCH

Many areas of this project could be improved by further work. Other edge detectors could be tested to find out how they affect segmentation. More features could

be extracted to better represent each ship class. Features could also be specified at a higher semantic level, as in [Ref. 2] where low-level information is grouped to identify masts, superstructures, and gun turrets. A more advanced difference calculation could improve performance as well. Studies such as [Ref. 8] and [Ref. 9] have proposed methods for a fast Hough transform, which could speed up segmentation significantly.

Another area for future study might be the construction of the comparison database. It would be useful to look at the results of building a database from non-FLIR images, since data may not be available for all of the ship types we would like to be able to identify and visual-spectrum images can be sharper. Finally, our algorithm does not currently handle images where the ship is very small or there is too much noise. A more robust extension that could work for these cases would be beneficial.

APPENDIX A. [MATLAB SOURCE CODE]

```
function [BW,mySegs2] = extractFeatures(I);

I = medfilt2(rgb2gray(I));
[BW,T] = edge(I,'canny');
[BW2,T2b] = edge(I,'canny',T*0.25);
load('roi2.mat');
IT = im2bw(I, 0.5);
[BWRows,BWCols] = size(BW);
[NBW,RBW,Segsfound2] = hough_and_segment(BW, 0, 0.03*(BWRows+BWCols));
RBW = bwmorph(RBW,'clean');
RBW = remove_small_regs(RBW, 9);
Regssofar = size(Segsfound2, 1);
[NBW2,RBW,Segsfound3] = hough_and_segment(RBW, Regssofar, 10);
NBW = NBW + NBW2;
Segsfound = [Segsfound2; Segsfound3];
temp3 = double(ROI2) + double(IT);
temp3 = temp3>0;
mySegs = centersAndEndpoints(Segsfound);
[mySegs2,segnums] = remainingSegs2(temp3,mySegs);
BW = drawLines(NBW,segnums);
figure, imshow(BW);
figure, imshow(NBW);
[BW,mySegs2] = transformImage(BW,mySegs2);
[BW,mySegs2] = tightenImage(BW,mySegs2);


function NBW = remove_small_regs(BW,Minlength)
% Remove small regions in a binary image
[CBW,Numregions] = bwlabel(BW,8);
NBW = BW;
for I=1:Numregions
  [YL,XL] = find(CBW==I);
  if (max(XL)-min(XL))<Minlength
    if (max(YL)-min(YL))<Minlength
      for J=1:size(XL,1)
        NBW(YL(J),XL(J)) = 0;
      end
    end
  end
end
```

```
function newSegs = centersAndEndpoints(seglist);

newSegs = [];
s = size(seglist);
for i=1:s(1)
  x1 = seglist(i,3);
  y1 = seglist(i,4);
  x2 = seglist(i,5);
  y2 = seglist(i,6);
  centerX = floor((x1 + x2)/2);
  centerY = floor((y1 + y2)/2);
  slope = seglist(i,1);
  r = seglist(i,2);
  numPix = seglist(i,7);
  segment = [x1 y1 x2 y2 centerX centerY slope r numPix];
  newSegs = [newSegs; segment];
end


function [newsegs,segnums] = remainingSegs2(ROI, segsfound);

s = size(segsfound);
newsegs = [];
segnums = [];
for i=1:s(1)
  if (ROI(segsfound(i,6),segsfound(i,5)) == 0)
    if (ROI(segsfound(i,2),segsfound(i,1)) == 0) | (ROI(segsfound(i,4),segsfound(i,3)) ==
0)
      newsegs = [newsegs; [segsfound(i,:) i]];
    else
      segnums = [segnums; i];
    end
  else
    segnums = [segnums; i];
  end
end


function BW = drawLines(NBW,segnums);

s = size(segnums);
BW = NBW;
for i=1:s(1)
  [x,y] = find(BW==segnums(i));
  sx = size(x);
```

```
  for j=1:sx(1)
    BW(x(j),y(j)) = 0;
  end
end
```

function [BWout,segsOut] = tightenImage(BW,segs);

```
[y,x] = find(BW>0);
mY = round(median(y));
stdY = round(std(y));
s = size(segs);
segsOut = [];
segnums = [];
for i=1:s(1)
  if (segs(i,6) < mY + 2.5*stdY) & (segs(i,6) > mY - 2.5*stdY)
    segsOut = [segsOut; segs(i,:)];
  else
    segnums = [segnums; segs(i,10)];
  end
end
BWout = drawLines(BW,segnums);
```

function [TBW,newSegs] = transformImage(NBW,segs);

```
BW = NBW>0;
theta = 70:110;
[R,xp] = radon(BW, theta);
[M,IX] = max(R);
[M2,IX2] = max(M);
thMax = 381 - IX2;
thMax = ((pi/180) * thMax);
theta = thMax;
TBW = zeros(size(BW));
[x,y,v] = find(BW);
x = x - 160;
y = y - 120;
s = size(x);
s2 = size(BW);
for i=1:s(1)
  xi = round(x(i)*cos(theta) - y(i)*sin(theta)) + 160;
  yi = round(y(i)*cos(theta)+x(i)*sin(theta)) + 120;
  if (xi > 0) & (yi > 0) & (xi < s2(1)) & (yi < s2(2))
    TBW(xi,yi) = NBW(x(i) + 160,y(i) + 120);
```

```
  end
end
s3 = size(segs);
newSegs = [];
for i=1:s3(1)
  %endpoints
  ns1 = round((segs(i,1)-160)*cos(theta)-(segs(i,1)-160)*sin(theta)) + 160;
  ns2 = round((segs(i,2)-120)*cos(theta)+(segs(i,2)-120)*sin(theta)) + 120;
  ns3 = round((segs(i,3)-160)*cos(theta)-(segs(i,3)-160)*sin(theta)) + 160;
  ns4 = round((segs(i,4)-120)*cos(theta)+(segs(i,4)-120)*sin(theta)) + 120;
  %center
  ns5 = round((segs(i,5)-160)*cos(theta)-(segs(i,5)-160)*sin(theta)) + 160;
  ns6 = round((segs(i,6)-120)*cos(theta)+(segs(i,6)-120)*sin(theta)) + 120;
  %orientation
  ns7 = segs(i,7) + theta;
  if ns7 > 2*pi
    ns7 = ns7 - 2*pi;
  end
  %r
  ns8 = segs(i,8);
  %#pixels
  ns9 = segs(i,9);
  %segment number
  ns10 = segs(i,10);
  newSegs = [newSegs; [ns1 ns2 ns3 ns4 ns5 ns6 ns7 ns8 ns9 ns10]];
end
```

function [NBW,RBW,Segsfound] =
hough_and_segment(BW,Baseregnum,Houghthresh)

```
% HOUGH_AND_SEGMENT Compute Hough transform and segment
% a binary image; returns residual binary image and a
% list of segments
% 3 outputs: Binary image of matches pixels.
% binary image of residual (unmatched) pixels,
% and list of segments found.
RBW = BW;
[BWRows,BWCols] = size(BW);
NBW = zeros(BWRows,BWCols);
Segsfound = [];
Regnum = Baseregnum;
theta = 0:179;
[R,P] = radon(BW,theta);
[HRows,HCols] = size(R);
R = [flipud(R(:,end-1)) flipud(R(:,end)) R flipud(R(:,1)) flipud(R(:,2))];
```

```
R = colfilt(R,[5 5],'sliding','columnIsolateMax',Houghthresh);
R = R(:,3:end-2);
[XDL,XTL,VL] = find(R);
% Note t and D here are defined differently in radon than in
% segsfound to come: they are referenced to center of image
TL = (pi/180) * (91-XTL);
DL = XDL - ((HRows+1)/2);
WL = [];
for I=1:size(TL,1)
  EPL = segment_endpoints_in_box(TL(I),DL(I),BWCols,BWRows);
  W = round(1000*(VL(I)/(10+distance(EPL(1:2),EPL(3:4)))));
  WL = [WL; W];
end
Peakinfo = sortrows([WL VL TL DL XTL XDL]);
Peakinfo = flipud(Peakinfo(1+end-min([200 size(TL,1)]):end,:));
if ~ isempty(Peakinfo)
  TL = Peakinfo(:,3);
  DL = Peakinfo(:,4);
  for K=1:size(TL,1)
    Peaksegs = [];
    EPL = segment_endpoints_in_box(TL(K),DL(K),BWCols,BWRows);
    if abs(EPL(1)-EPL(3)) >= abs(EPL(2)-EPL(4))
      SFlag = 0;
      Z0 = round(min(EPL(1),EPL(3)));
      Zend = round(max(EPL(1),EPL(3)));
    else
      SFlag = 1;
      Z0 = round(min(EPL(2),EPL(4)));
      Zend = round(max(EPL(2),EPL(4)));
    end
    [ORXL,ORYL,Z] =
find_clump(RBW,TL(K),DL(K),BWCols,BWRows,Z0,Zend,SFlag);
    RFlag = 0;
    while ~RFlag
      RFlag = (Z>=Zend);
      [RXL,RYL,Z] =
find_clump(RBW,TL(K),DL(K),BWCols,BWRows,Z,Zend,SFlag);
      Dist = point_cluster_dist(ORXL,ORYL,RXL,RYL);
      if Dist<3
        RXL = [ORXL; RXL];
        RYL = [ORYL; RYL];
      elseif size(ORXL,1) > 9
        [FE,NXL,NYL] = fit_and_extremes(ORXL,ORYL);
        if FE(3)>0 & size(NXL,1)>9
          if distance(FE(3:4),FE(5:6))>8
```

```
            Peaksegs = [Peaksegs; FE];
            Regnum = Regnum+1;
            for I=1:size(NXL,1)
              RBW(NYL(I),NXL(I)) = 0;
              NBW(NYL(I),NXL(I)) = Regnum;
            end
          end
        end
      end
      ORXL = RXL;
      ORYL = RYL;
    end
    Segsfound = [Segsfound; Peaksegs];
    if ~ isempty(Peaksegs)
      NewPeaksegs = Peaksegs;
    end
  end
end

function [XL,YL,Z] = find_clump(BW,T,D,Cols,Rows,Z0,Zend,SFlag)
% FIND_CLUMP: Finds connected group of pixels in binary image BW
% that lie along line defined by (T,D). Z represents the
% coordinate (X or Y) of greater extent within box.
Z = Z0;
XL = [];
YL = [];
ST = sin(T);
CT = cos(T);
EFlag = 0;
XC = (Cols+1)/2;
YC = (Rows+1)/2;
EFlag == 0;
if SFlag == 0 & Z < Zend
  while Z <= Zend & EFlag < 2
    Y = round(YC-(D/CT)+((Z-XC)*ST/CT));
    B1 = BW(Y,Z);
    if Y<Rows
      B2 = BW(Y+1,Z);
    else
      B2 = 0;
    end
    if Y>1
      B3 = BW(Y-1,Z);
    else
      B3 = 0;
```

```
    end
    if ~(B1|B2|B3)
      if EFlag == 1
        EFlag = 2;
      else
        Z = Z+1;
      end
    else
      if B1
        XL = [XL; Z];
        YL = [YL; Y];
      end
      if B2
        XL = [XL; Z];
        YL = [YL; Y+1];
      end
      if B3
        XL = [XL; Z];
        YL = [YL; Y-1];
      end
      EFlag = 1;
      Z = Z+1;
    end
  end
elseif SFlag == 1 & Z < Zend
  while Z <= Zend & EFlag < 2
    X = round(XC+(D/ST)+((Z-YC)*CT/ST));
    B1 = BW(Z,X);
    if X<Cols
      B2 = BW(Z,X+1);
    else
      B2 = 0;
    end
    if X>1
      B3 = BW(Z,X-1);
    else
      B3 = 0;
    end
    if ~(B1|B2|B3)
      if EFlag == 1
        EFlag = 2;
      else
        Z = Z+1;
      end
    else
```

```
      if B1
        XL = [XL; X];
        YL = [YL; Z];
      end
      if B2
        XL = [XL; X+1];
        YL = [YL; Z];
      end
      if B3
        XL = [XL; X-1];
        YL = [YL; Z];
      end
      EFlag = 1;
      Z = Z+1;
    end
  end
end

function D = point_cluster_dist(XL1,YL1,XL2,YL2);
% Approximate distance between point clusters in the same
% narrow corridor from the distance between closest pair
% of endpoints
if (isempty(XL1) | isempty(XL2))
  D = 1000;
else
  EPS1 = quick_endpoints(XL1,YL1);
  EPS2 = quick_endpoints(XL2,YL2);
  D1 = distance(EPS1(1:2),EPS2(1:2));
  D2 = distance(EPS1(1:2),EPS2(3:4));
  D3 = distance(EPS1(3:4),EPS2(1:2));
  D4 = distance(EPS1(3:4),EPS2(3:4));
  D = min([D1 D2 D3 D4]);
end

function EPS = quick_endpoints(XL,YL)
Xmin = min(XL);
Xmax = max(XL);
Ymin = min(YL);
Ymax = max(YL);
if abs(Xmax-Xmin)>abs(Ymax-Ymin)
  EP1 = Xmin;
  EP3 = Xmax;
  for I=1:size(XL)
    if XL(I)==Xmin
      EP2 = YL(I);
```

```
    end
    if XL(I)==Xmax
      EP4 = YL(I);
    end
  end
else
  EP2 = Ymin;
  EP4 = Ymax;
  for I=1:size(XL)
    if YL(I)==Ymin
      EP1 = XL(I);
    end
    if YL(I)==Ymax
      EP3 = XL(I);
    end
  end
end
EPS = [EP1 EP2 EP3 EP4];


function isomax = columnIsolateMax(subarray,thresh);

s = size(subarray);
isomax = zeros(1,s(2));
for i=1:s(2)
  if ((subarray(13,i) >= max(subarray(:,i))) & subarray(13,i) >= thresh)
    isomax(i) = subarray(13,i);
  end
end


function EPL = segment_endpoints_in_box(T,D,Cols,Rows)
ST = sin(T);
CT = cos(T);
XC = (Cols+1)/2;
YC = (Rows+1)/2;
if abs(CT)>0.001
  Y0 = YC - (D/CT);
  YD = ST*(XC-1)/CT;
  LY = Y0 - YD;
  RY = Y0 + YD;
else
  LY = 10000;
  RY = 10000;
end
```

```
if abs(ST)>0.001
  X0 = XC + (D/ST);
  XD = CT*(YC-1)/ST;
  UX = X0 - XD;
  DX = X0 + XD;
else
  UX = 10000;
  DX = 10000;
end
PL = [];
if (LY >= 0.99) & (LY <= Rows+0.01)
  PL = [PL; 1 LY];
end
if (RY >= 0.99) & (RY <= Rows+0.01)
  PL = [PL; Cols RY];
end
if (UX >= 0.99) & (UX <= Cols+0.01)
  PL = [PL; UX 1];
end
if (DX >= 0.99) & (DX <= Cols+0.01)
  PL = [PL; DX Rows];
end
if size(PL,1)>1
  EPL = [PL(1,:) PL(2,:)];
else
  EPL = [PL(1,:) PL(1,:)];
end
if size(PL,1)>2 & distance(PL(1,:),PL(2,:))<0.03
  EPL = [PL(1,:) PL(3,:)];
end
```

```
function [Answer,NXL,NYL] = fit_and_extremes(XL,YL)
% Fit_and_extremes: Compute linear regression and endpoints
% for a set of points represented by X and Y lists
ON = size(XL,1);
[T,D] = lsfit_points(XL,YL);
ST = sin(T);
CT = cos(T);
NXL = [];
NYL = [];
for I=1:size(XL,1)
  if abs((-ST*XL(I))+(CT*YL(I))-D) < 1.01
    NXL = [NXL; XL(I)];
    NYL = [NYL; YL(I)];
```

```
  end
end
N = size(NXL,1);
if N>1
  if ON<N
    [T,D] = lsfit_points(NXL,NYL);
    ST = sin(T);
    CT = cos(T);
  end
  R = (CT*NXL)+(ST*NYL);
  Rmax = [R(1) 1];
  Rmin = [R(1) 1];
  for I=1:N
    if R(I) > Rmax(1)
      Rmax = [R(I) I];
    else
      if R(I) < Rmin(1)
        Rmin = [R(I) I];
      end
    end
  end
  I1 = Rmax(2);
  I2 = Rmin(2);
  Answer = [T D NXL(I1) NYL(I1) NXL(I2) NYL(I2) N];
else
  Answer = [0 0 0 0 0 0 0];
  NXL = [];
  NYL = [];
end
```

function [T,D] = lsfit_points(XL,YL)

```
% LSFIT_POINTS: Fit least-squares line through points
% defined by X and Y lists.
Ones = ones(size(XL,1),1);
if (max(XL)-min(XL))>(max(YL)-min(YL))
  BM = [Ones XL] \ YL;
  T = atan(BM(2));
  D = BM(1)/sqrt((BM(2)*BM(2))+1);
else
  BM = [Ones YL] \ XL;
  T = acot(BM(2));
  D = BM(1)/sqrt((BM(2)*BM(2))+1);
  if T>0
    D = -D;
```

```
  end
end


function D = distance(P1,P2);
% DISTANCE: Between 2 points
DX = P2(1)-P1(1);
DY = P2(2)-P1(2);
D = sqrt((DX*DX)+(DY*DY));


function difference = compareImages(BW1in,BW2in,segs1,segs2,alfa1,alfa2,alfa3);

BW1 = BW1in>0;
BW2 = BW2in>0;
boxes1 = stdBoxCenters(BW1,segs1);
boxes2 = stdBoxCenters(BW2,segs2);
[pix1,orient1] = countBoxPixels(boxes1);
[pix2,orient2] = countBoxPixels(boxes2);
[diffP,diffO] = calcDiff(pix1,pix2,orient1,orient2)
moment1 = calcMoment(BW1,3)
moment2 = calcMoment(BW2,3)
diffM = abs(moment1 - moment2)

difference = alfa1 * diffP + alfa2 * diffO + alfa3 * diffM;

function DB = addToDB(BW,segs,DBin);

boxes = stdBoxCenters(BW,segs);
[pix,orient] = countBoxPixels(boxes);
moment = calcMoment(BW,3);
temp = [reshape(pix,1,25) reshape(orient,1,100) moment];
DB = [DBin; temp];

function [order,values] = compareToDB(BW,segs,DB);

alfa1 = 1;
alfa2 = 10;
alfa3 = 5;
BW1 = BW>0;
boxes1 = stdBoxCenters(BW1,segs);
[pix1,orient1] = countBoxPixels(boxes1);
moment1 = calcMoment(BW1,3);
diffList = [];
s = size(DB);
```

```
for i=1:s(1)
  pix2 = reshape(DB(i,1:25),5,5);
  orient2 = reshape(DB(i,26:125),5,5,4);
  moment2 = DB(i,126);
    [diffP,diffO] = calcDiff(pix1,pix2,orient1,orient2);
  diffM = abs(moment1 - moment2);
  difference = alfa1 * diffP + alfa2 * diffO + alfa3 * diffM;
  diffList = [diffList; difference];
end
[values,order] = sort(diffList);
```

function STDBW = addStdevLines(BW);

```
[x,y] = find(BW>0);
mX = round(median(x));
mY = round(median(y));
stdX = round(std(x));
stdY = round(std(y));
s = size(BW);

STDBW = BW;

if (mX + stdX/2) <= s(1)
  STDBW(round(mX + stdX/2),:) = 1;
  if (mX + (3/2 * stdX)) <= s(1)
    STDBW(round(mX + (3/2 * stdX)),:) = 1;
    if (mX + (5/2 * stdX)) <= s(1)
      STDBW(round(mX + (5/2 * stdX)),:) = 1;
    end
  end
end
if (mX - stdX/2) > 0
  STDBW(round(mX - stdX/2),:) = 1;
  if (mX - (3/2 * stdX)) > 0
    STDBW(round(mX - (3/2 * stdX)),:) = 1;
    if (mX - (5/2 * stdX)) > 0
      STDBW(round(mX - (5/2 * stdX)),:) = 1;
    end
  end
end
if (mY + stdY/2) <= s(2)
  STDBW(:,round(mY + stdY/2)) = 1;
  if (mY + (3/2 * stdY)) <= s(2)
    STDBW(:, round(mY + (3/2 * stdY))) = 1;
```

```
    if (mY + (5/2 * stdY)) <= s(2)
      STDBW(:,round(mY + (5/2 * stdY))) = 1;
    end
  end
end
if (mY - stdY/2) > 0
  STDBW(:,round(mY - stdY/2)) = 1;
  if (mY - (3/2 * stdY)) > 0
    STDBW(:, round(mY - (3/2 * stdY))) = 1;
    if (mY - (5/2 * stdY)) > 0
      STDBW(:,round(mY - (5/2 * stdY))) = 1;
    end
  end
end
```

function [pixels,orient] = countBoxPixels(boxes);

```
pixels = zeros(5,5);
orient = zeros(5,5,4);
s = size(boxes);
totalP = 0;
for i=1:s(1)
  pixels(boxes(i,2),boxes(i,1)) = pixels(boxes(i,2),boxes(i,1)) + boxes(i,5);
    orient(boxes(i,2),boxes(i,1), getOrient(boxes(i,4))) =
orient(boxes(i,2),boxes(i,1),getOrient(boxes(i,4))) + boxes(i,5);
    totalP = totalP + boxes(i,5);
end
for i=1:5
  for j=1:5
    for k=1:4
      orient(i,j,k) = orient(i,j,k)/totalP;
    end
    pixels(i,j) = pixels(i,j)/totalP;
  end
end
```

function o = getOrient(angle);

```
if (angle > (3*pi/4)) | (angle <= -(3*pi/4))
  o = 1;
else if (angle > pi/4)
    o = 2;
  else if (angle > -pi/4)
```

```
      o = 3;
    else if (angle > -(3*pi/4))
      o = 4;
    else
      angle
    end
  end
end
```

function regions = stdBoxCenters(BW, seglist);

```
[x,y] = find(BW>0);
mX = round(median(x));
mY = round(median(y));
stdX = round(std(x));
stdY = round(std(y));
s = size(seglist);
regions = [];
for i=1:5
  for j=1:5
    for k=1:s(1)
      if ((seglist(k,5) < (mY + round((i - 2.5) * stdY))) & (seglist(k,5) >= (mY + round((i
- 3.5) * stdY))) & (seglist(k,6) < (mX + round((j - 2.5) * stdX))) & (seglist(k,6) >= (mX +
round((j - 3.5) * stdX))))
        regions = [regions; [i j k seglist(k,7) seglist(k,9)]];
      end
    end
  end
end
```

function [diffP,diffO] = calcDiff(pix1,pix2,orient1,orient2);

```
diffMat = zeros(5,5);
diffOrient = zeros(5,5,4);
for i=1:5
  for j=1:5
    diffMat(i,j) = abs(pix1(i,j)-pix2(i,j));
    for k=1:4
      diffOrient(i,j,k) = abs(orient1(i,j,k)-orient2(i,j,k));
    end
  end
end
```

```
diffO = sum(sum(sum(diffOrient)));
diffP = sum(sum(diffMat>0));


function moment = calcMoment(BW,nth);

[x,y] = find(BW);

n = size(x);
n = n(1);
moment = 0;
mu = mean(x);
for i=1:n
  moment = moment + ((x(i) - mu)^nth);
end
moment = abs(moment / n);
moment = moment^(1/nth);
```

APPENDIX B. [EQUATIONS]

HOUGH TRANSFORM

A straight line in the (x,y) plane can be represented as:

$$s = x\cos\theta + y\sin\theta$$

where s is the perpendicular distance from the origin and θ is the orientation of the line. The Hough transform of this line is a single point in the (s,θ) plane. All of the points on the line map to a single location. In an edge image, we can count the number of edge pixels which map to each location in the (s,θ) plane. Local maxima of the count function correspond to straight line segments in the edge image.

MOMENTS

The k^{th} moment of a set of pixels about its mean x value is defined as:

$$\sqrt[k]{\frac{\sum_{i=1}^{n}(x_i - \bar{x})^k}{n}}$$

where the x_i are the x-coordinates of all non-zero pixels, x-bar is the mean of x_i, and n is the number of pixels.

THIS PAGE INTENTIONALLY LEFT BLANK

APPENDIX C. [IMAGES]

Arleigh Burke Images

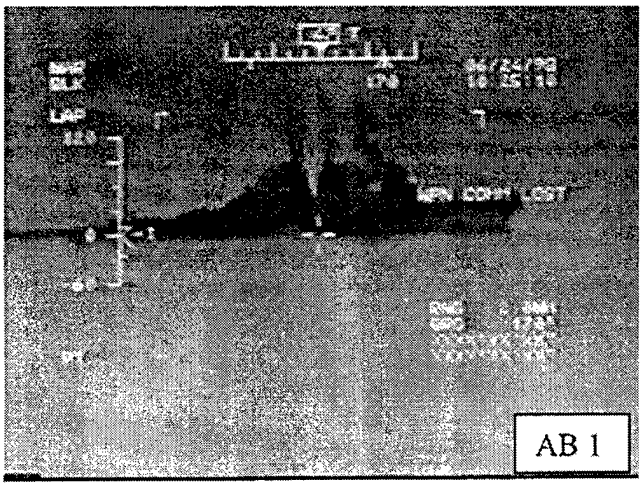

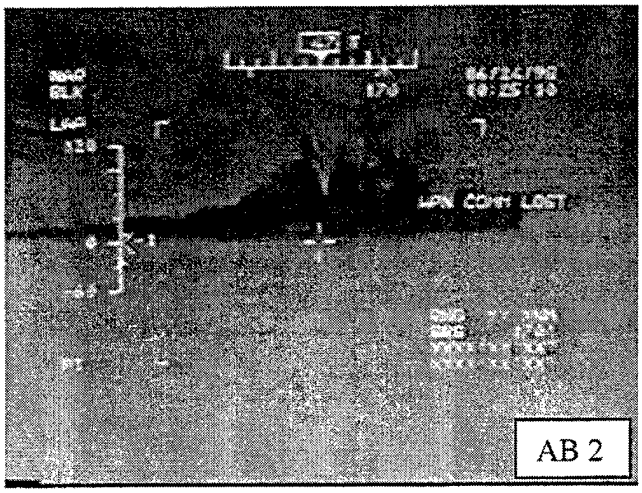

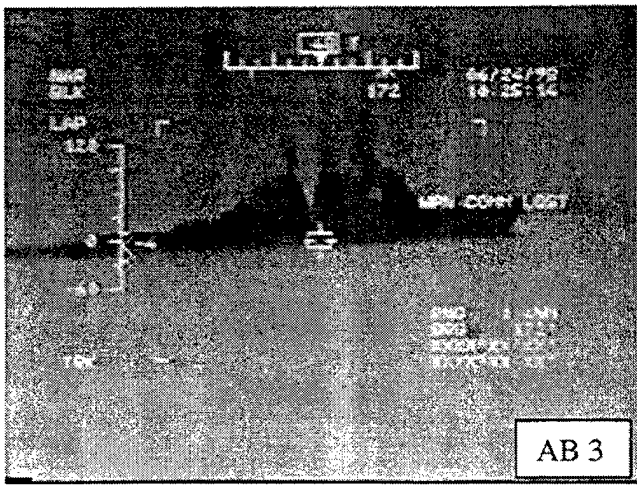

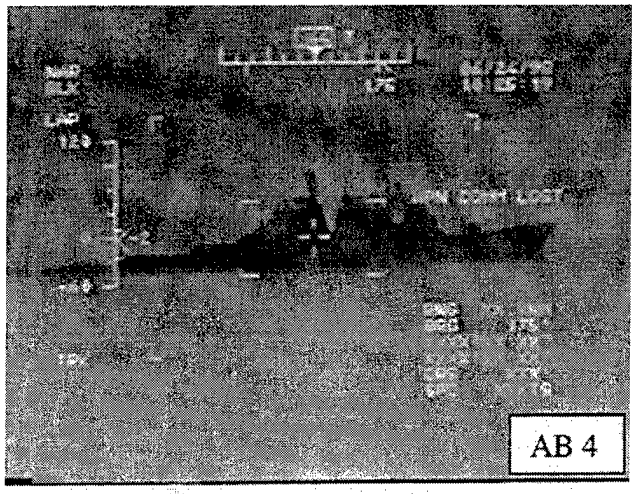
AB 4

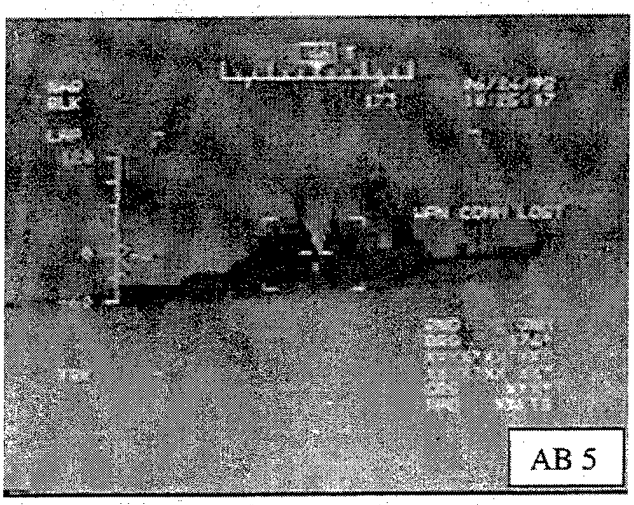
AB 5

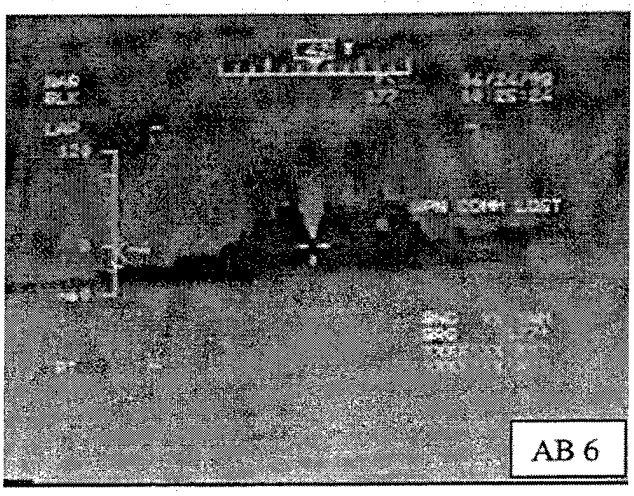
AB 6

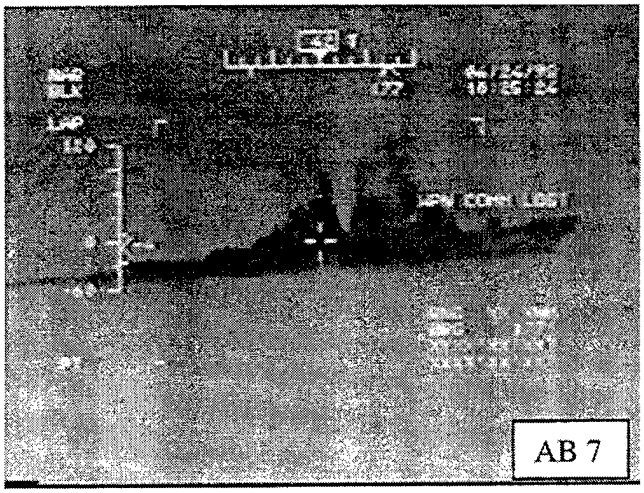
AB 7

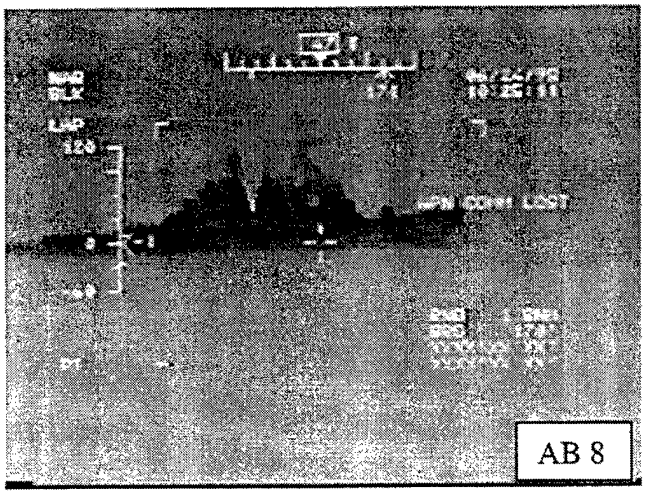
AB 8

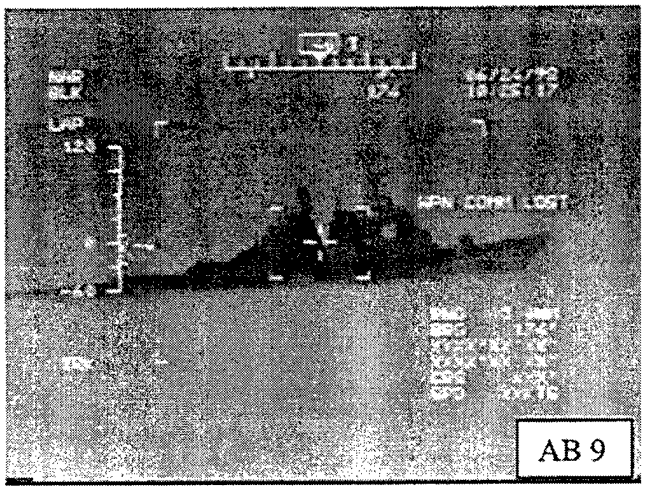
AB 9

Aircraft Carrier Images

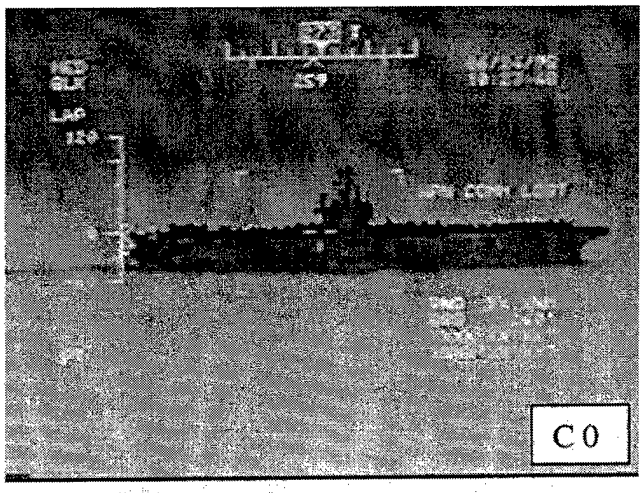

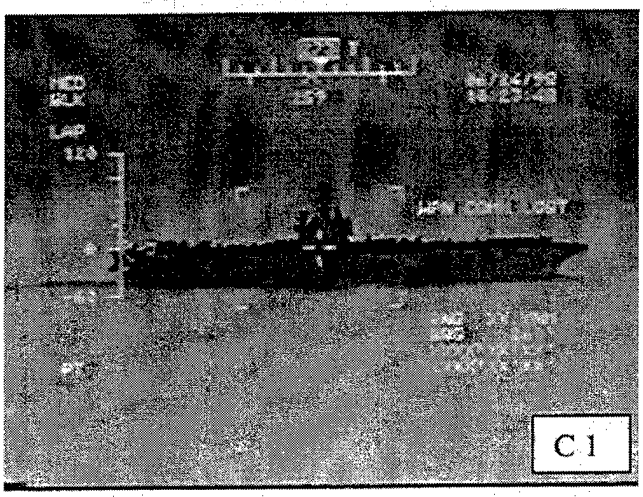

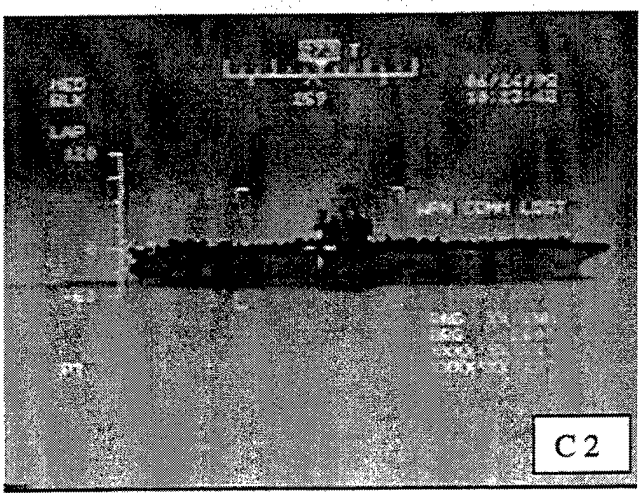

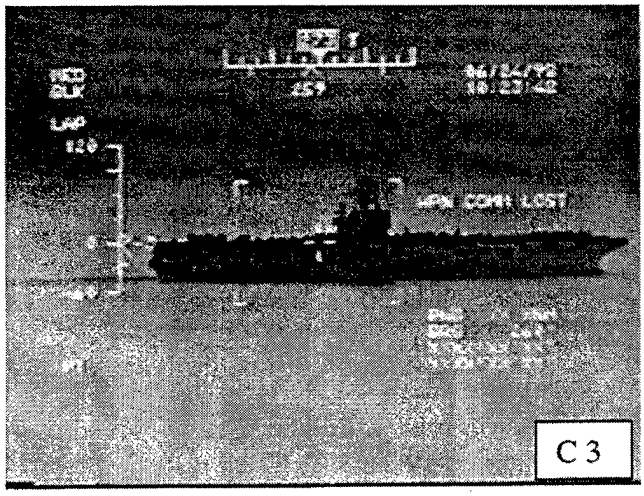
C 3

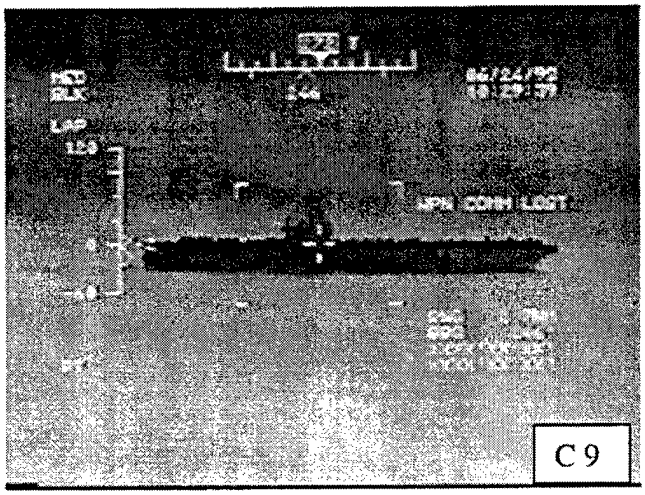
C 9

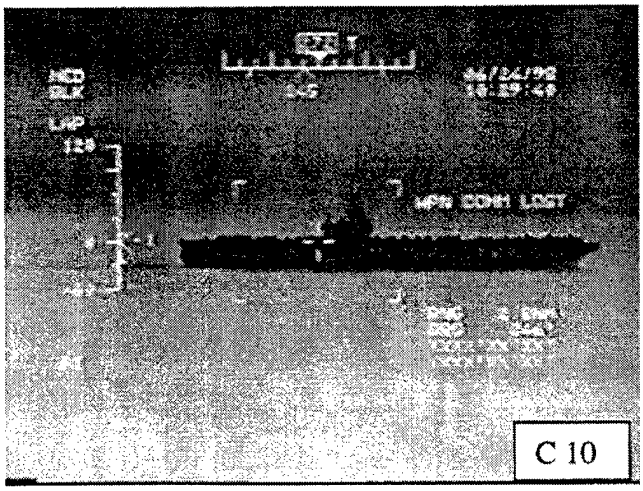
C 10

Spruance and PTG Images

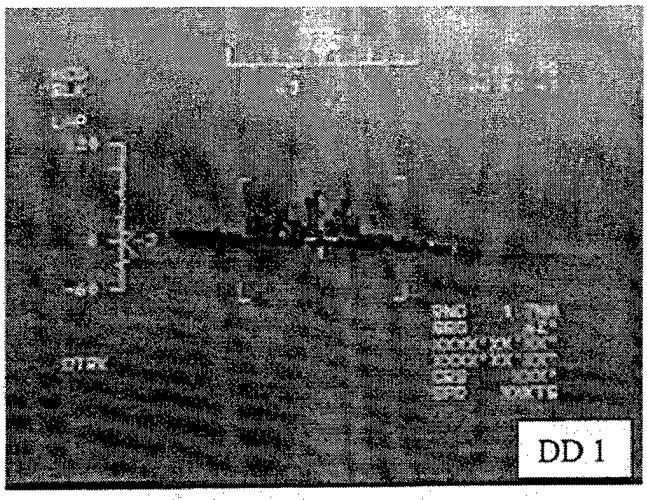

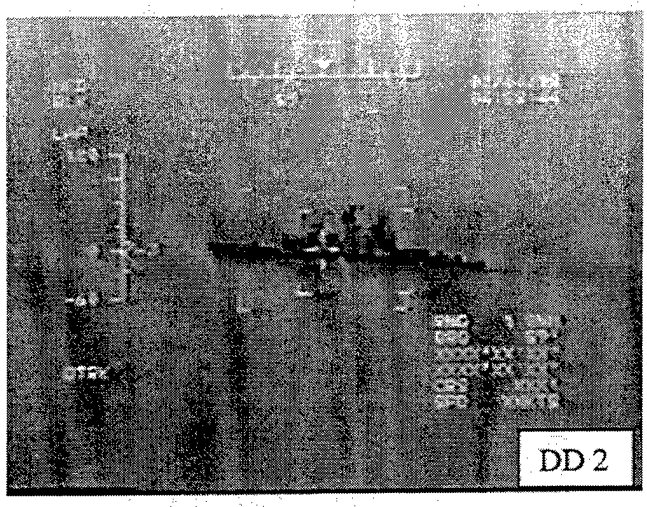

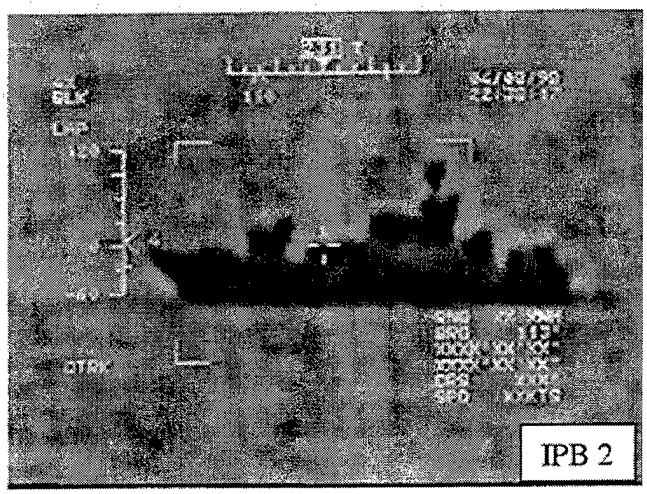

LIST OF REFERENCES

1. M. J. Bizer, "A picture-descriptor extraction program using ship silhouettes," Master's Thesis, Naval Postgraduate School, Monterey, California, June 1989.

2. *Jane's All the World's Fighting Ships 1985-1986,* Jane's Publishing Inc., pp. 216-217, 1986.

3. P. Sinha, F. Chen, and R. Home, "Recognition and location of shapes in the Hough parameter space," IEEE Colloquium on Hough Transforms, pp. 11/1 – 11/4, 1993.

4. C. Chau and W. Siu, "Generalized dual-point Hough transform for object recognition," Proceedings, 1999 International Conference on Image Processing, vol. 1, pp. 560-564, 1999.

5. J. Illingworth and J. Kittler, "The Adaptive Hough Transform," *IEEE Transactions on Pattern Analysis and Machine Intelligence,* vol. PAMI-9, pp. 690-698, 1987.

6. C.C. Lin and R. Chellappa, "Classification of partial 2-D shapes using Fourier descriptors," *IEEE Transactions on Pattern Analysis and Machine Intelligence,* vol. PAMI-9, pp. 686-690, 1987.

7. S. A. Dudani, K. J. Breeding, and R.B. McGhee, "Aircraft identification by moment invariants," *IEEE Transactions on Computers,* vol. C-26, pp. 39-46, 1977.

8. C. Chau and W. Siu, "New dominant point detection for image recognition," ISCAS '99 – 1999 IEEE International Symposium on Circuits and Systems, pp. 102-105, 1999.

9. A. Khashman and K. M. Curtis, "A novel image recognition technique for 3-dimensional objects," 13th International Conference on Digital Signal Processing Proceedings, vol.2, pp. 535-538, 1997.

10. N. C. Rowe, "System design for automatic updating of terrain databases from satellite imagery," *http://www.cs.nps.navy.mil/people/faculty/rowe/spaceprop.html.*

THIS PAGE INTENTIONALLY LEFT BLANK

BIBLIOGRAPHY

K. Arimura and N. Hagita, "Feature space design for image recognition with image screening," Proceedings of the 13th International Conference on Pattern Recognition, vol. 2, pp. 261-265, 1996.

D. Casasent, "Optical pattern recognition and AI algorithms and architectures for ATR and computer vision," *Image Pattern Recognition: Algorithm Implementations, Techniques and Technology*, Francis J. Corbett, Editor, Proc. SPIE 755, pp. 84-93, 1987.

S. R. Dubois, and F. H. Glanz, "An autoregressive model approach to two-dimensional shape classification," *IEEE Transactions on Pattern Analysis and Machine Intelligence,* vol. PAMI-8, pp. 55-65, 1986.

M. A. Green, et. al., "Target recognition in infra-red imagery using neural networks and machine learning," Third International Conference on Artificial Neural Networks, pp. 21-25, 1993.

H. Kauppinen, T. Seppanen, and M. Pietikainen, "An experimental comparison of autoregressive and Fourier-based descriptors in 2D shape classification," *IEEE Transactions on Pattern Analysis and Machine Intelligence,* vol. 17, pp. 201-207, 1995.

S. Nishio, H. Takano, T. Maejima, and T. Nakamura, "A study of image recognition system," Third International Conference on Image Processing and its Applications, pp. 112-116, 1989.

D. Prevost et. al, "Rotation, scale and translation invariant pattern recognition using feature extraction," *Optical pattern Recognition VIII,* David P. Casasent, Tien-Hsin Chao, Editors, Proc. SPIE 3073, pp. 255-263, 1997.

F. Sadjadi, "Automatic object recognition: critical issues and current approaches," *Automatic Object Recognition,* Firooz A. Sadjadi, Editor, Proc. SPIE 1471, pp. 303-313, 1991.

X. Wenan, "The enhanced vision system and recognition algorithm of ground targets images," Proceedings, CIE International Conference of Radar, pp. 644-647, 1996.

THIS PAGE INTENTIONALLY LEFT BLANK

INITIAL DISTRIBUTION LIST

1. Defense Technical Information Center.....2
   8725 John J. Kingman Rd., STE 0944
   Ft. Belvoir, Virginia 22060-6218

2. Dudley Knox Library.....2
   Naval Postgraduate School
   411 Dyer Rd.
   Monterey, California 93943-5101

3. Chairman, Code CS.....1
   Computer Science Department
   Naval Postgraduate School
   Monterey, California 93943-5000

4. Dr. Neil Rowe.....1
   Computer Science Department, Code CS/Rp
   Naval Postgraduate School
   Monterey, California 93943-5100

5. Jessica Herman.....1
   104 River Road
   Merrimac, Massachusetts 01860